Dielectric properties of phase separated polymer solids: 2. Butanediol terephthalate–poly (tetramethylene oxide terephthalate) copolymers

Alastair M. North, Richard A. Pethrick and Alexander D. Wilson*

Department of Pure and Applied Chemistry, University of Strathclyde, 295 Cathedral Street, Glasgow G1 1XL, UK

(Received 10 October 1977; revised 13 January 1978)

The low frequency dielectric behaviour of copolymers of butanediol terephthalate with poly(tetramethylene oxide terephthalate) is reported. Comparison of the theories for interfacial polarization with experimental dielectric observations highlights the role of domain boundary conduction in such polar polymers.

INTRODUCTION

In a previous paper[1] the authors observed that the low frequency dielectric properties of styrene–butadiene–styrene regular block copolymers could be interpreted using an extension of the simplest theories for interfacial polarization. Morphologies predicted using the theories were in good agreement with those actually observed. In particular the dielectric properties could be explained in terms of a regular array of two clearly-defined phases, and there was no necessity to postulate a diffuse interphase boundary region of electrical conductivity differing from (greater than) that of either non-polar phase. In this study, observations are extended to two phase polar systems where the morphology, although not so perfectly regular as in the styrene–butadiene systems, can be easily characterized.

The polymers chosen for study were polyethers–polyesters formed between butanediol terephthalate (4GT) and poly(tetramethylene oxide terephthalate) (PTMGT) and have the structure:

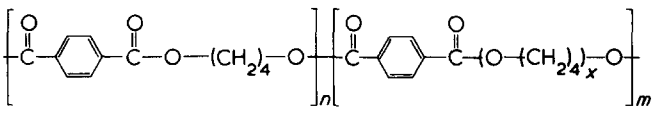

The commercial elastomer 'Hytrel' has essentially this structure, with a small amount of butanediol isophthalate (4GI) included. The copolymers are synthesized by melt transesterification of butanediol, poly(tetramethylene oxide) and dimethyl terephthalate mixed in proportions to give 4GT blocks of a size suitable for crystallization[2,3]. The preferential crystallization of these 'hard' blocks forms a three-dimensional structure in which 4GT crystallites are separated by 'soft' amorphous regions of PTMGT[3,4]. The phase-separated morphology of these copolymers has been characterized using small-angle X-ray diffraction, transmission and scanning electron microscopy, differential scanning calorimetry and mechanical relaxation measurements[3–5]. No evidence of PTMGT crystallization was reported from X-ray studies[4,5]. Dynamic mechanical properties of polyurethane/polyether copolymers indicate that for x = 14 a single α-relaxation is observed while for x = 28 two processes occur, attributed to amorphous and crystalline phase relaxations[11]. The morphologies obtained in these measurements are significantly different from those reported both for the SBS copolymers and semicrystalline homopolymers, and so allow further critical comparison of the theories of interfacial polarization with experimental observation.

EXPERIMENTAL

Materials

The samples studied were provided by Du Pont de Nemours and Co., Wilmington, Delaware, USA, in the form of melt crystallized sheets. These polymers are marketed under the trade name 'Hytrel' and have M_n values between 2.5 and 3.0 x 10^4, the poly(tetramethylene oxide) moiety having a degree of polymerization (x above) of 14. The samples were vacuum annealed at 420K for 24 h and then stored over P_2O_5 under vacuum until used. The measured densities and glass transition temperatures are reported in *Table 1*, and agree with the literature data[6].

Dielectric measurements

The dielectric measurements were performed using the techniques described previously[1]. Contact with the samples was made by colloidal Aquadag electrodes. Uniaxially orientated samples of one of the copolymers (sample 1) were prepared by drawing the specimen used for the initial study at low rates of extension at 300K. The subsequent dielectric measurements were confined to temperatures below 300K so

* Present address: Proctor and Gamble Ltd, Newcastle Technical Centre (2), Whitley Road, Longbenton, Newcastle-upon-Tyne, NE12 9TS, UK.

0032–3861/78/1908–0923$02.00

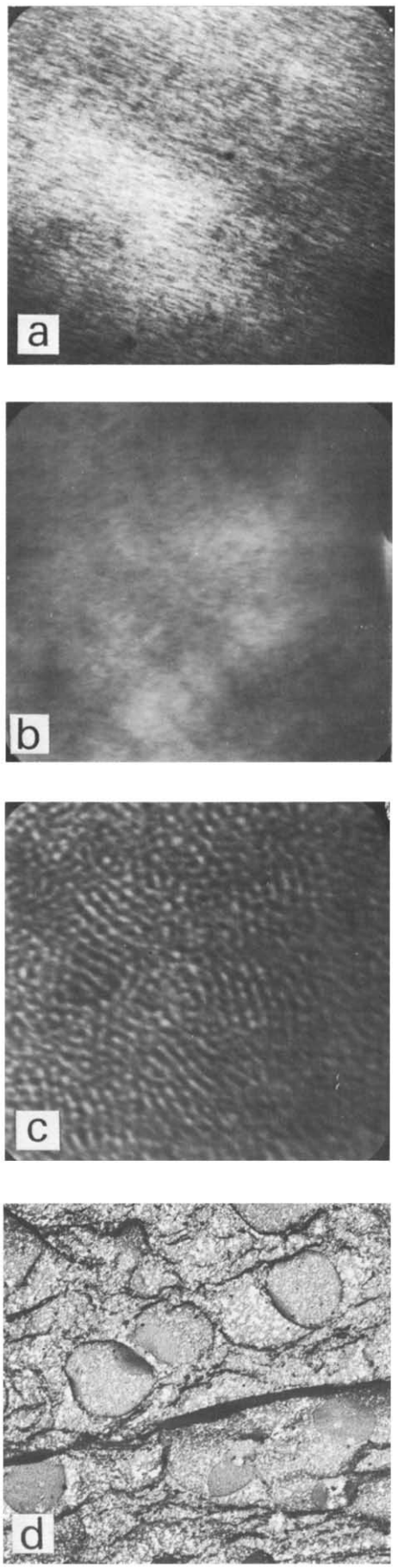

Figure 1 Transmission electron micrographs of 'Hytrel' polymers: (a) sample S1, magnification 80 000; sample S2, magnification 40 000; (c) sample S3, iodine stained magnification 50 000; (d) sample S3, magnification 3000

as to avoid possible morphological changes. The drawn samples are designated in terms of their draw ratio, λ, defined as the drawn length/original length.

Electron microscopy

Transmission micrographs were obtained as described previously[1] and scanning micrographs were obtained by Dr P. F. Millington of the Bioengineering Department of this University, using a Cambridge 600 Scanning Electron Microscope.

RESULTS AND DISCUSSION

Electron microscopy and sample morphology

The transmission electron micrographs of thin sections of the copolymers PS1 and S2, cut perpendicular to the sample surface and stained by exposure to 0.1% phosphotungstic acid solution in *Figures 1a* and *1b* appear as a series of parallel dark and light regions which may be ellipsoidal domains of axial ratio $(a/b) = 10$. These domains are comparable in size to those previously reported for these copolymers[4,5]. Sample S3 exhibited a very indistinct morphology which on staining with iodine developed a textured structure (*Figure 1c*). This type of morphology resembles that observed in polyurethane–ether block copolymers[7], the iodine being excluded from the crystallite regions and staining the amorphous phase block (*Figure 1c*).

At low magnification (*Figure 1d*) the copolymer (sample 3) exhibits a grain structure of approximately 3 μm size. Spherulites of similar size have been reported previously[5]. The copolymers clearly exhibit a phase-separated morphology, although neither the detail nor the regularity are so clearly defined as in the styrene–butadiene styrene copolymers. Morphological modelling based on X-ray and electron microscopy studies of the Hytrel copolymers[4,5] indicates that the preferred structure is one in which the 4GT crystallites are of approximately rectangular cross-section with axial ratios of twenty or less and lengths of up to 200 nm. In such structures the 4GT chains are oriented perpendicular to the major crystallite axis, and are distributed throughout several adjacent crystallites. In practice this ideal morphology may not be achieved since chain mobility and the effects of entanglement during melt crystallization lead to 'hard' segments being found within the 'soft' amorphous regions. The net result of the various interactions between hard and soft blocks together with the exclusion of short chains from the crystalline regions, is the formation of a sheath-like structure. The volume fraction of crystalline material (v_c) may be estimated from the density using the relation

$$v_c = (\rho - \rho_A)/(\rho_C - \rho_A) \quad (1)$$

where ρ is the density, ρ_C is the crystallite density (1.43×10^3 kg/m^3)[8] and the amorphous phase is assumed to have a density, $\rho_A = 1.05 \times 10^3$ kg/m^3, which is the mean of those of the poly(tetramethylene oxide) (0.98×10^3 kg/m^3)[9] and the isophthalate ester (1.24×10^3 kg/m^3). Values of v_c calculated using equation (1) are presented in *Table 1*.

High frequency dielectric relaxation

Unorientated samples. The dielectric spectra of the three copolymers show a peak (α) in the region 250–300K with a

Table 1 Characteristics of the 'Hytrel' copolymers

Sample code	4GT (wt %)	4GT Block length	4GI (wt %)	T_g(K)	Density (10^3 kg/m^3)	Crystallite volume fraction, v_c
S1	38	6	15	209 ± 3	1.146	0.26
S2	60	8	0	225 ± 3	1.189	0.37
S3	72	24	7	265 ± 3	1.241	0.50

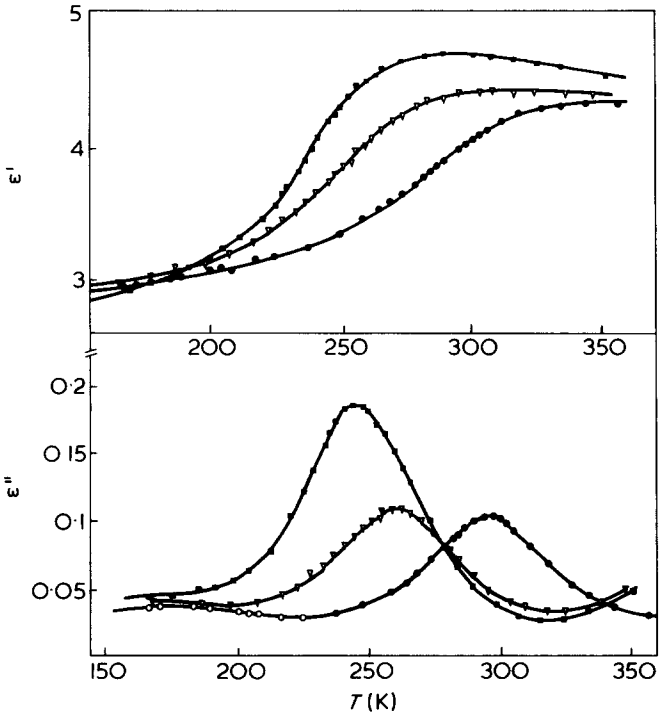

Figure 2 A.c. dielectric spectra at 1.34 kHz. □, S1; ▽, S2; ●, S3

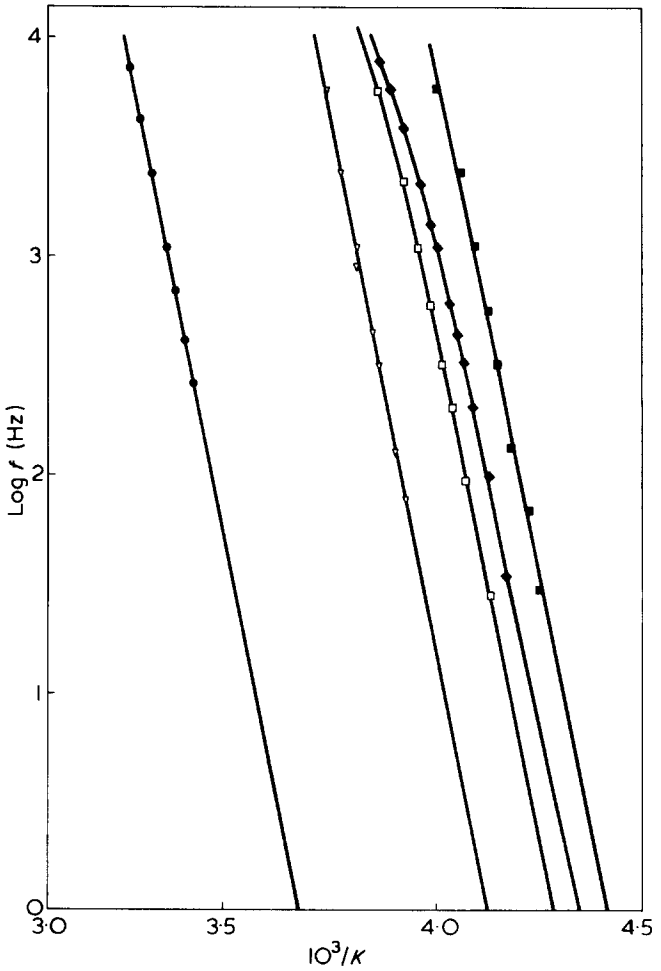

Figure 3 Arrhenius plots for α relaxation: ●, S3; ▽, S2; ■, SI (λ-1 = 0); ◆, S1 (λ-1 = 0.77); □, S1, (λ-1 = 1.23)

smaller broad partly resolved peak (β) at lower temperatures than the main feature (*Figure 2*). The apparent activation energy for the main relaxation process, 190 ± 20 kJ/mol (*Figure 3*) is consistent with relaxation due to the cooperative micro-Brownian motion of the chain backbone in the amorphous region, and is similar to that found for the corresponding processes, in other polymers containing poly(tetramethylene oxide) or PTMGT moieties[5,11]. The temperature of maximum loss increases with increasing 'hard' segment content and is higher for block copolymers than for the poly(tetramethylene oxide) homopolymers. This behaviour is consistent with an increase in motional constraint placed on the chain in the amorphous region by the increasing crystallinity of the sample[14] and by the 'anti-plasticization' effect expected[5] when 4GI and 4GT segments occur at high concentrations in the amorphous region.

Since both 4GI and 4GT are more polar than PTMGT, the relaxation magnitude does not vary in a simple manner as the 'hard' segment content is increased. The decrease in $\Delta\epsilon$ expected on lowering the PTMGT content is countered at high 4GT–4GI levels by the increased polarity of the isophthalate (*Figure 2*). Calculations of the amorphous phase permittivity ϵ_α, using a model[15] applicable to semicrystalline polymers, confirms that the amorphous phase of S3 is considerably more polar than that in the other polymers (*Table 2*).

Table 2 Electrical characteristics of the amorphous regions

	Permittivity data (1 kHz at 298.2K)			Conductivity data (Ω^{-1} m^{-1}) at 298.2K		
Sample	ϵ	ϵ_c	ϵ_a	σ	σ_c	σ_c
S1	4.7	5.5	2.8	3.2×10^{-15}	7.7×10^{-15}	10^{-19}
S2	4.4	5.6	2.8	6.1×10^{-16}	2.3×10^{-15}	10^{-19}
S3	4.35	6.4	2.8	8.0×10^{-18}	4.4×10^{-17}	10^{-19}

The lower temperature relaxation corresponds in frequency–temperature to a process in similar polymers ascribed[5,11] to librational motion of the chain segments. This process is complicated by contributions from both amorphous and crystalline regions[16,17].

Uniaxially oriented samples. The effects of uniaxial orientation on the high temperature relaxation process are summarized in *Table 3.*

The observed decrease in ϵ''_{max} with draw ratio is consistent with an increase in population of the *trans* configuration of the poly(tetramethylene oxide) moiety[18,19] which is compatible with the observed increase of density and hence of molecular alignment in the amorphous region. These observations are similar to those reported for the effects of uniaxial orientation of the dielectric behaviour of similar polymers[20–22].

Low frequency dielectric behaviour

D.c. transient studies. The normalized time dependent discharge traces in *Figure 4,* show well-defined break points characteristic of relaxation processes within the time scale of observation. Subtraction of the long time component of the decay curve and Fourier transformation[23,24] of the data lead to the dielectric relaxation spectra shown in *Figure 5.* Arrhenius plots of the d.c. conductivity and relaxation frequency data are shown in *Figure 6* which also includes data on the isochronal (100 sec) extrapolated absorption current for S2. The relaxation parameters at 298.3K are given in *Table 4.*

It should be noted that as a result of truncation of the short time discharge ($t \leqslant 1$ sec), the data at 304.7 and 298.4K for S1 become distorted on transformation, and the relaxa-

Table 3 Effect of uniaxial orientation on the α-relaxation of SI

λ^{-1}	Density (10^3kg/m^3)	T_g(K)	T_{max}(K) (1 kHz)	ϵ''_{max}
0.00	1.146	209 ± 3	243.7	0.186
0.53	1.151	211 ± 3	247 3	0.166
0.77	1.152	211 ± 3	249.4	0 160
1.23	1.155	215 ± 3	252.4	0.152

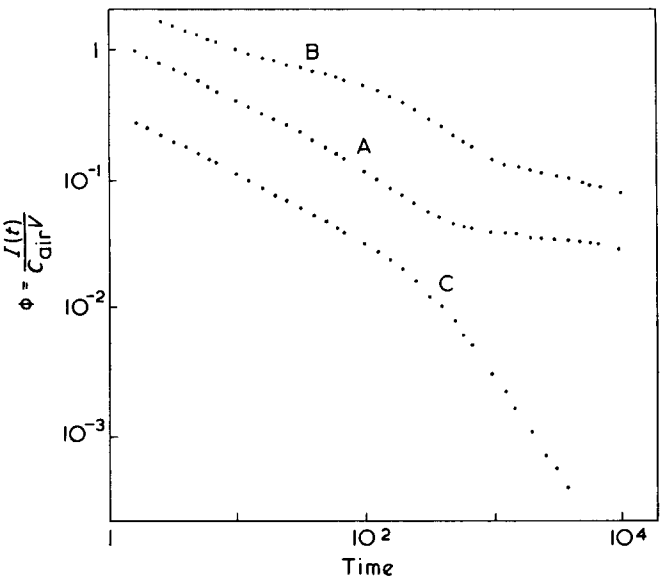

Figure 4 Discharge traces from d.c. transient experiments A, S1 (273K); B, S2 (294K); C, S3 (301K)

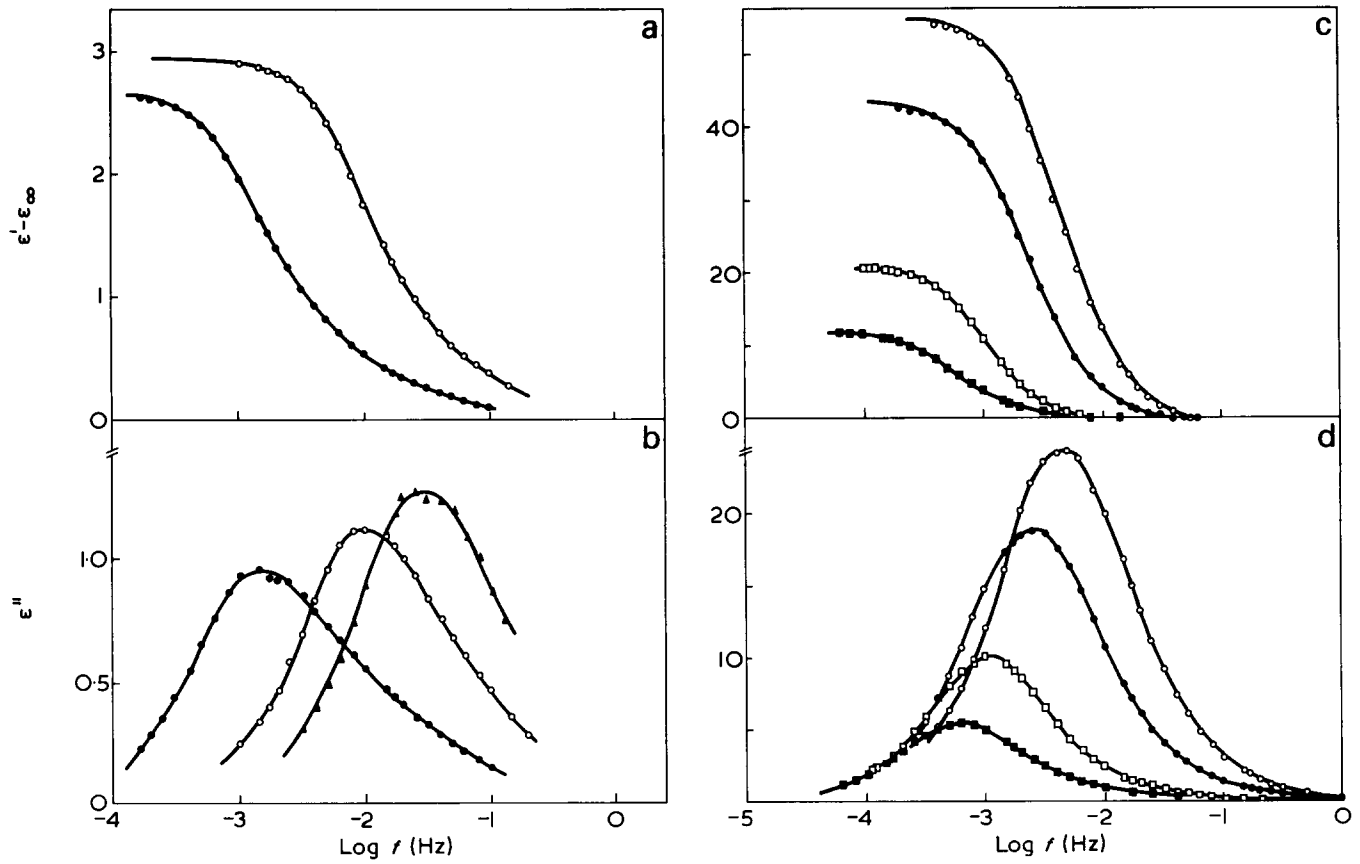

Figure 5 (a) Resolved low frequency relaxation, S1 (λ − 1 = 0): ●, 273.2K; ○, 297.3K; △, 304.7K. (b) Resolved low frequency relaxation, S1 (λ − 1 = 0.77): ●, 265.7K; ○, 273.2K; ▲, 298.4K; ■, 304.4K

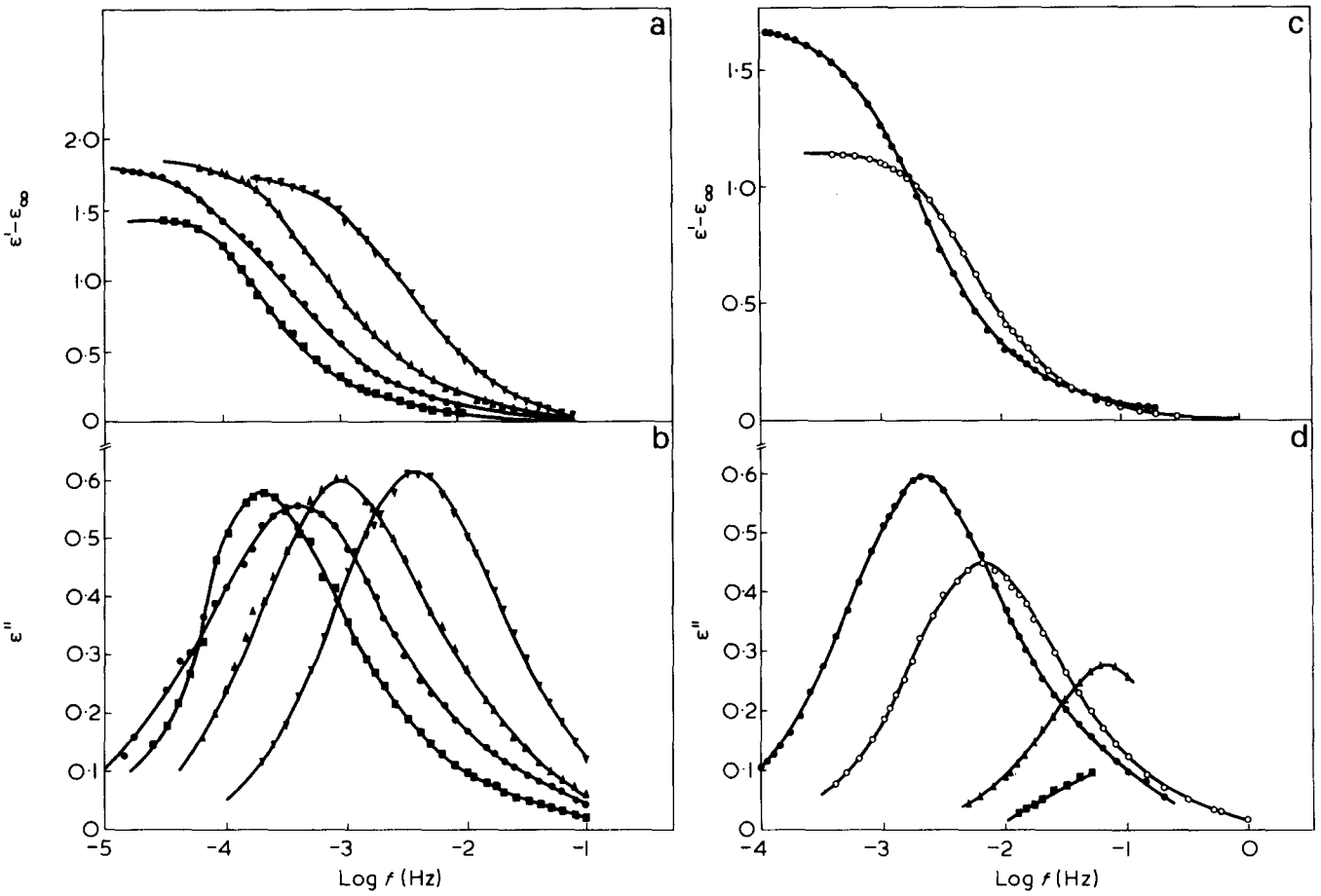

Figure 6 (a) Resolved low frequency relaxation, S2. ■, 294.2K; □, 300.0K; ●, 307.8K; ○, 313.4K. (b) Resolved low frequency relaxation, S3: ■, 296.6K; ●, 300.8K; ▲, 305.4K; ▽, 312.8K

Table 4 Low frequency relaxation data for the copolymer at 298.2K

Sample	ϵ_∞	ϵ_0	$\Delta\epsilon_{exp}$	τ_{exp}(sec)	σ_{exp} (Ω^{-1} cm^{-1})	Activation energy for relaxation (kJ/mol)	Activation energy for conduction (kJ/mol)
S1	4.7	7.7	3.0	10.6	3.2×10^{-15}	72 ± 15	82 ± 10
S2	4.4	22.2	17.8	167.5	6.1×10^{-16}	83 ± 5	77 ± 5
S3	4.35	6.35	2.0	589.5	8.0×10^{-18}	142 ± 10	144 ± 10

tion frequencies are reduced from their true values. Consequently relaxation frequencies obtained using the Hamon approximation[25] were used for construction of the Arrhenius plots (*Figure 7*). This procedure is not expected to lead to significant error provided the shape of the relaxation does not change appreciably with temperature. On this assumption, which in this case is justified, f_{max}(Hamon)/f_{max}(true) will be a constant[26].

D.c. conductivities and absorption currents. Comparison of the data presented in *Tables 1* and *2* indicates that the d.c. conductivity decreases as the crystallite volume fraction increases, indicating that the amorphous phase is the more highly conducting of the two. This observation is in agreement with the predictions of model calculations[15,28] (*Table 2*). The apparent similarity in the activation energies for conduction in samples S1 and S2 supports the hypothesis of identical amorphous structures. The lower charge mobility of S3 is attributed to a higher 4GT content in this sample which will both decrease the segmental mobility and increase the charge trapping probability.

Resolved low frequency relaxations

It is clear from the frequency–temperature loci of the low frequency relaxations (*Table 4*) that the observed features are inconsistent with dipolar relaxation processes associated with either the amorphous or crystalline domains. A plot of the relationship between the relaxation frequency and the d.c. conductivity (*Figure 8*) is approximately linear, indicating that the relaxation is due to bulk charge transport The mechanism could involve localized carrier hopping between adjacent trapping sites in the amorphous regions or an interfacial polarization involving the bulk morphology.

The idealized hopping model[29] predicts relaxation times which are similar to those observed experimentally, while the intertrap separation, d, as calculated from the observed relaxation magnitude is larger than has been reported for

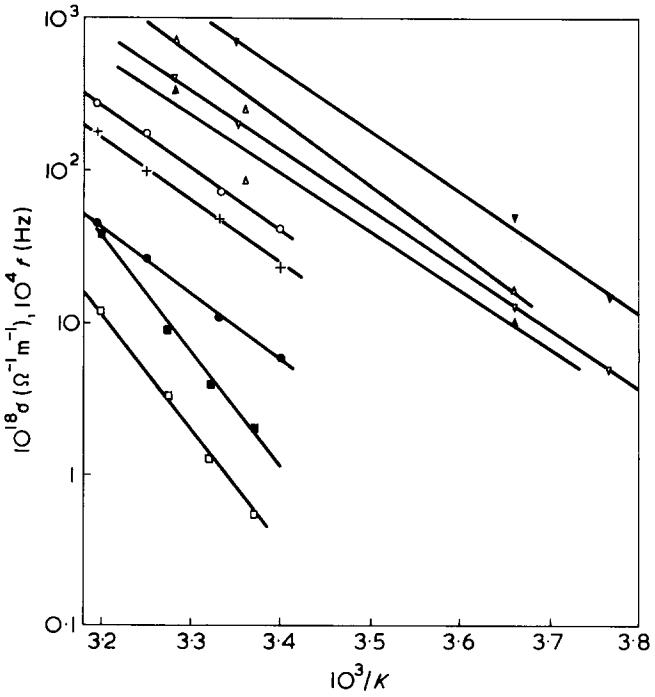

Figure 7 Arrhenius plots for d.c. conduction (□, ○, △, ▽) and f_{max} of the low frequency process (■, ●, ▲, ▼). The lines are least squares fits. □, ■, S3; ○, ●, S2; △, ▲, S1 (λ − 1 = 0); ▽, ▼, S1 (λ − 1 = 0.77); X

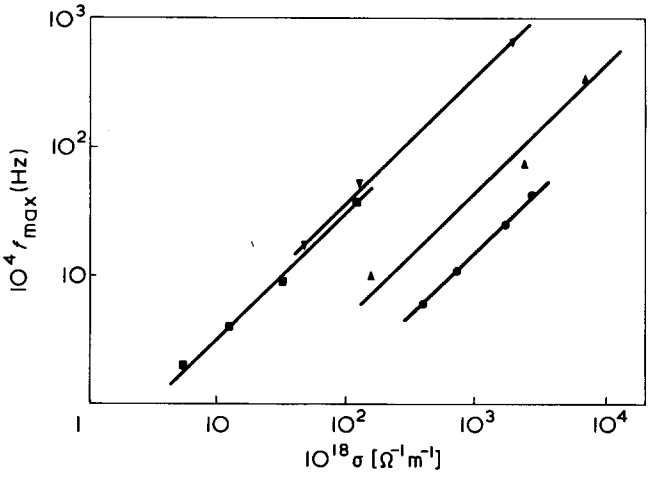

Figure 8 The relationship between d.c. conductivity and relaxation frequency for the low frequency process. The lines are of unit negative slopes. ■, S3; ●, S2; ▲, S1 (λ − 1 = 0); ▼, S1 (λ − 1 = 0.77)

other polymers[30–32]. Consequently, these low frequency relaxations are best ascribed to interfacial polarization.

Application of Maxwell–Wagner–Sillars (MWS) theory. As a first approximation we consider the amorphous phase to be a continuous matrix in which are dispersed non-conducting crystalline prolate ellipsoids. The dielectric properties may be calculated as a function of the ellipsoid axial ratio for three morphologies, respectively: (a) *a*-axis parallel[33]; (b) *a*-axis perpendicular[33]; and (c) randomly orientated to the electric field[34].

The calculated quantities (*Tables 5a–5d*) are not in good agreement with the experimental observations (*Table 4*).

Although the amorphous phase appears continuous (*Figure 1c*) and it may be argued $v_a = v_c = 0.5$ in sample S3, it would be equally valid to assume that the matrix was the non-conducting crystalline phase (*Table 5d*). The calculated relaxation time is then in good agreement with experiment for axial ratios of around unity, but the magnitude of the relaxation is overestimated.

Although the poor agreement between theory and experiment may be due in part to the use of the MWS relations at volume fractions strictly outside their range of validity, use of models expected to hold for higher loadings[35] gives an even poorer fit to the data. Also the idealized situation of isolated ellipsoids does not reflect the real morphology which more closely resembles an interpenetrating network of two semi-continuous phases. A further approximation implicit in the simple MWS approach ignores the possibility that the region of polarizable charge may be diffuse[36–38].

Alternative approaches to the low frequency interfacial loss. Consideration of charge transport in semicrystalline polymer systems[27,30–32] leads one to the conclusion that migration is controlled not only by the bulk mobility, but also by the occurrence of traps at interfacial boundaries. Evidence for this hypothesis comes from the effect of impurity molecules, which concentrate at boundaries, on the polymer conductivity[36,40–43]. It is therefore not unreasonable to suggest that crystallites with appreciable surface conductivity may markedly influence the low frequency relaxation properties. Introduction of a frequency independent surface conductivity with $\sigma_a \gg \sigma_c$ leaves $\Delta\epsilon$ unchanged but decreases τ from its MWS value and therefore does not improve agreement between theory and experiment.

The effects of a time-dependent surface conductivity can be estimated[44] assuming that the crystallites are rods with dimensions (a = 100 and b = 10 nm) which are independent of copolymer composition (*Table 6*). The surface mobility η^S is assumed to decrease with crystallite volume fraction. The number of relaxing charge carriers N_r may be obtained from the surface charge carrier density σ', and the calculated crystallite surface area. The bulk charge carrier mobility η^B is expected to be greater than η^S since the 'surface' charge carriers are constrained in a diffuse interfacial layer of reduced molecular freedom. Assuming that η^B equals $2\eta^S$ we may make a crude estimation of the number of charge carriers in the bulk conduction process, $N_\sigma = v_a n_a$, where n_a is the charge carrier density in the amorphous phase. It should be noted that the values of N_r/N_σ are less than 2 (*Table 6*) and the n_a are of the expected order of magnitude for polar polymers[40].

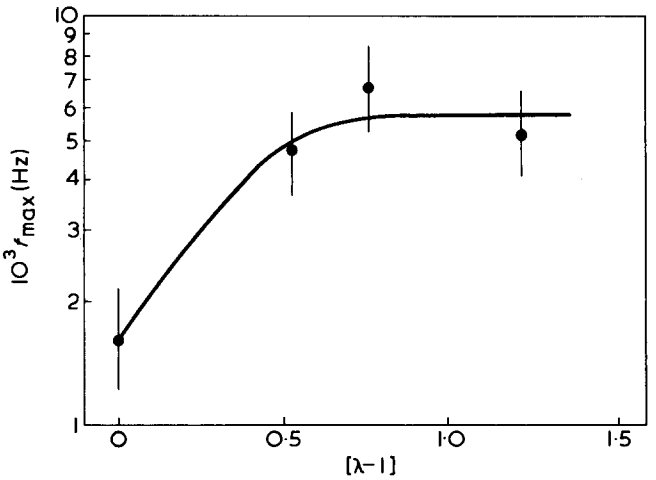

Figure 9 Dependence of f_{max} at 273.2K on uniaxial orientation. The low frequency process, S1

Table 5 Relaxation parameters calculated using the MWS model

Axial ratio (a/b)	Parallel		Perpendicular		Random			
	ϵ_∞	$\Delta\epsilon$	ϵ_∞	$\Delta\epsilon$	ϵ_∞	$\Delta\epsilon$	τ_a (sec)	τ_b (sec)
Sample 1:								
100	4.798	0	4.642	0.422	4.694	0.281	0.632	0.820
10	4.793	0.006	4.642	0.406	4.695	0.273	0.637	0.815
1	4.701	0.183	4.701	0.183	4.701	0.183	0.737	0.737
0.1	4.479	2.606	4.780	0.22	4.679	0.883	1.197	0.650
0.01	4.407	5.703	4.796	0.002	4.666	1.902	1.496	0.634
1*	4.695	0.045						
Sample S2:								
100	4.564	0	4.371	0.419	4,435	0.279	2.156	2.650
1	4.442	0.195	4.442	0.195	4.442	0.195	2.441	2.441
0.01	4.098	3.229	4.561	0.003	4.407	1.078	3.914	2.159
0†	4.088	3.480	4.564	0	4.405	1.160	3.989	2.155
1*	4.432	0.139						
Sample S3:								
100	4.600	0	4.306	0.316	4.404	0.211	128.7	147.5
1	4.414	0.162	4.414	0.162	4.414	0.162	140.0	140.0
0.01	3.911	1.617	4.596	0.002	4.368	0.540	183.3	128.9
1*	4.503	0.106						
Sample S3, randomly oriented amorphous ellipsoids in a crystalline matrix:								
100	4.31	515					22 650	295
1	4.28	6.9					405	405
0.1	4.36	383					186	7243
1*	5.06	17.34						

* Calculated using Hanai–Bruggeman equations (*Table 1b*, ref 1); † layered dielectric

Table 6 Calculated parameters for frequency dependent surface conductivity

Sample	η^S (m^2/r sec)	σ' (m^{-2})	Crystallite surface area (m^2)	N_R (m^{-3})	η^B (m^2/v sec)	η_A (m^{-3})	N_σ (m^3)	N_R/N_σ
S1	4.6×10^{-15}	1.36×10^{14}	1.04	1.41×16^{22}	$9{,}2 \times 10^{-15}$	5.4×10^{22}	4.0×10^{22}	0.35
S2	2.9×10^{-16}	3.9×10^{13}	1.48	5.8×10^{22}	5.8×10^{-16}	3.4×10^{23}	2.1×10^{23}	0.28
S3	8.3×10^{-17}	6.6×10^{13}	2.0	1.32×10^{22}	1.66×10^{-16}	1.7×10^{22}	8.5×10^{21}	1.55

Table 7 Low frequency properties of SI at 273.2K under uniaxial orientation

λ^{-1}	10^{16} (Ω^{-1} m^{-1})	$10^3 f_{max}$ (Hz)	$\Delta\epsilon$	E_σ (kJ/mol)	Ef (kJ/mol)
0.0	1.62	1.5	2.65	82 ± 5	72 ± 10
0.53	1.18	4.6	0.70	–	–
0.77	1.32	6.6	1.135	77 ± 5	76 ± 50
1.23	0.89	4.8	0.44	–	–

Alteration of the crystallite dimensions of the $\eta^S - \eta^B$ relationship does not significantly alter these conclusions.

It is apparent that the inclusion of a frequency-dependent surface conductivity may, in principle, account for the low frequency relaxations in the copolymers. However since the theory[44] relies on values of the mobility, and charge carrier density of the amorphous phase which are not readily determinable from experiment, the explanation must be considered as qualitative.

Effects of axial orientation on the low frequency loss. As expected, the uniaxial orientation of the copolymers alters the low frequency density on elongation and indicates greater molecular order in the amorphous regions and is expected to lead to a reduced charge carrier mobility and therefore a lower conductivity. However the conduction process will also reflect changes in the sample morphology as a result of rupture and deformation of the crystallites on drawing. The net result of the stretching process is to produce elongation and alignment of the crystallites in the direction of draw, with an increase in the angles, γ_i, subtended by the electric field on the crystallite axes. Quantitative evaluation of the MWS equations becomes impossible since the $\cos^2 \gamma_i$ coefficients are not known exactly. Qualitatively, deformation of a random array of non-conducting crystallites in a 'conducting' amorphous matrix leads to an increase in the number of orientations in which the major axis and the electric field are at right angles, (analogous to the perpendicular rods or parallel lamellae in the *a*-axis notation used previously). This and surface conductivity models[43,44] predict the observed decrease in both the relaxation time and relaxation magnitude upon drawing.

CONCLUSIONS

It appears from this study of polar polymers that the surface conductivity approach provides a more realistic description

of interfacial polarization in the present systems. The restricted applicability of the simple MWS approach was demonstrated in the previous study of very regular SBS copolymers, and this highlights the fact that in polar polymers charge trapping and mobility within a diffuse interfacial region have a dominant effect on the low frequency dielectric properties.

REFERENCES

1 North, A. M., Pethrick, R. A. and Wilson, A. D. *Polymer* 1978, **19**
2 Hoeschele, G. K. and Witsiepe, W. K. *Angew. Makromol. Chem.* 1973, **29–30**, 267
3 Witsiepe, W. K. *Polym. Prepr.* 1972, **13**, 588
4 Cella, R. J. *J. Polym. Sci. (Polym. Symp.)* 1973, **42**, 727
5 Buck, W. H. and Cella, R. J. *Polym. Prepr.* 1973, **14**, 98
6 Shen, M., Mehra, U., Niinomi, M., Koberstein, J. T. and Cooper, S. L. *J. Appl. Phys.* 1974, **45**, 4182
7 Koutsky, J. A., Hien, N. V. and Cooper, S. L. *Polym. Lett.* 1970, **8**, 353
8 Alter, U. and Bonart, R. *Colloid Polym. Sci.* 1976, **254**, 348
9 Warner, F. P., Brown, D. S. and Wetton, R. E. *J. Chem. Soc. (Faraday Trans. 2)* 1976, **72**, 1064
10 Conix, A. and Van Kerpel, R. *J. Polym. Sci.* 1959, **40**, 521
11 Huh, D. S. and Cooper, S. L. *Polym. Eng. Sci.* 1971, **11**, 369
12 Wetton, R. E. and Williams, G. *Trans. Faraday Soc.* 1965, **61**, 2132
13 Wetton, R. E., Fielding-Russell, G. S. and Fulcher, J. U. *J. Polym. Sci. (C)* 1970, **30**, 219
14 Read, B. E. *Polymer* 1962, **3**, 529
15 Looyenga, H. *Physica* 1965, **31**, 401
16 Yamafuji, K. and Ishida, Y. *Kolloid Z. Z. Polym.* 1961, **183**, 15
17 Ishida, Y., Yamafuji, K., Ito, H. and Takayanagi, M. *Kolloid Z. Z. Polym.* 1962, **184**, 97
18 Adam, G. and Gibbs, J. H. *J. Chem. Phys.* 1965, **43**, 139
19 Ward, I. M. 'Mechanical Properties of Solid Polymers', Wiley–Interscience, London, 1971
20 Ito, E. and Hatakeyama, T. *J. Polym. Sci. (Polym. Phys. Edn)* 1974, **12**, 1477
21 Ito, E., Sawamura, K. and Aito, S. *Colloid Polym. Sci.* 1975, **253**, 480
22 Ito, E., Okajima, S., Sasabe, H. and Saito, S. *Kolloid Z. Z. Polym.* 1973, **251**, 577
23 Dev, S. B., North, A. M. and Pethrick, R. A. *Adv. Mol Relaxation Processes* 1972, **4**, 159
24 Dev, S. B., North, A. M. and Reid, J. C. in 'Dielectric Properties of Polymers' (Ed. F. E. Karasz), Plenum Press, New York, 1972, p 217
25 Hamon, B. V. *Proc. Inst. Electr. Eng. (London)* 1952, **99**, 115
26 Kita, Y. and Koizumi, N. *Adv. Mol. Relaxation Processes* 1975, **7**, 13
27 Sazhin, B. I. and Podosenova, N. G. *Polym. Sci. USSR* 1964, **6**, 162
28 Wintle, H. J. *J. Non-crystalline Solids* 1974, **15**, 471
29 Carnochan, P. and Pethig, R. *J. Chem. Soc. (Faraday Trans. 1)* 1976, **72**, 2355
30 Davies, D. K. *J. Phys. (D)* 1972, **5**, 162
31 Kryszewski, M., Kasica, H., Patora, J. and Piotrowski, J. *J. Polym. Sci. (C)* 1970, **30**, 243
32 Anborski, L. E. *J. Polym. Sci.* 1962, **62**, 331
33 Sillars, R. W. *J. Inst. Electr. Eng.* 1937, **80**, 378
34 Fricke, H. *J. Phys. Chem.* 1953, **57**, 934
35 Hanai, T. *Kolloid Z.* 1960, **171**, 23
36 Reiser, A., Lock, M. W. B. and Knight, J. *Trans. Faraday Soc.* 1969, **65**, 2168
37 Kosaki, M., Olshima, H. and Ieda, M. *J. Phys. Soc. Jpn* 1970, **29**, 1012
38 Dukhin, S. S. and Shilov, V. N. 'Dielectric Phenomena and the Double Layer in Disperse Systems and Polyelectroytes', Wiley, New York, 1974
39 Kargin, V. A., Podosenova, N. G., Andrianova, G. P. and Sazhin, B. I. *Polym. Sci. USSR* 1967, **9**, 323
40 Barker, R. E. and Thomas, C. R. *J. Appl. Phys.* 1964 **35**, 3203
41 Partridge, R. H. *J. Polym. Sci. (B)* 1967, **5**, 205
42 Lewis, T. J. and Taylor, D. M. *J. Phys. (D)* 1972, **5**, 1664
43 Sakai, T., Miyasaka, K. and Ishikawa, K. *J. Polym. Sci. (A-2)* 1972, **10**, 253
44 Takashima, S. *Adv. Chem. Ser.* 1967, **63**, 232
45 Kryszewski, M. *J. Polym. Sci. (Polym. Symp.)* 1975, **50**, 359